Alteration of the Diastereoselectivity of 3-Methylaspartate Ammonia Lyase by Using Structure-Based Mutagenesis

ARTICLE *in* CHEMBIOCHEM · SEPTEMBER 2009

Impact Factor: 3.09 · DOI: 10.1002/cbic.200900311 · Source: PubMed

CHEMBIOCHEM

DOI: 10.1002/cbic.200900311

Alteration of the Diastereoselectivity of 3-Methylaspartate Ammonia Lyase by Using Structure-Based Mutagenesis

Hans Raj,[a] Barbara Weiner,[b] Vinod Puthan Veetil,[a] Carlos R. Reis,[a] Wim J. Quax,[a] Dick B. Janssen,[c] Ben L. Feringa,[b] and Gerrit J. Poelarends*[a]

3-Methylaspartate ammonia-lyase (MAL) catalyzes the reversible amination of mesaconate to give both (2*S*,3*S*)-3-methylaspartic acid and (2*S*,3*R*)-3-methylaspartic acid as products. The deamination mechanism of MAL is likely to involve general base catalysis, in which a catalytic base abstracts the C3 proton of the respective stereoisomer to generate an enolate anion intermediate that is stabilized by coordination to the essential active-site Mg^{II} ion. The crystal structure of MAL in complex with (2*S*,3*S*)-3-methylaspartic acid suggests that Lys331 is the only candidate in the vicinity that can function as a general base catalyst. The structure of the complex further suggests that two other residues, His194 and Gln329, are responsible for binding the C4 carboxylate group of (2*S*,3*S*)-3-methylaspartic acid, and hence are likely candidates to assist the Mg^{II} ion in stabilizing the enolate anion intermediate. In this study, the importance of Lys331, His194, and Gln329 for the activity and stereoselectivity of MAL was investigated by site-directed mutagenesis. His194 and Gln329 were replaced with either an alanine or arginine, whereas Lys331 was mutated to a glycine, alanine, glutamine, arginine, or histidine. The properties of the mutant proteins were investigated by circular dichroism (CD) spectroscopy, kinetic analysis, and ^{1}H NMR spectroscopy. The CD spectra of all mutants were comparable to that of wild-type MAL, and this indicates that these mutations did not result in any major conformational changes. Kinetic studies demonstrated that the mutations have a profound effect on the values of k_{cat} and k_{cat}/K_M; this implicates Lys331, His194 and Gln329 as mechanistically important. The ^{1}H NMR spectra of the amination and deamination reactions catalyzed by the mutant enzymes K331A, H194A, and Q329A showed that these mutants have strongly enhanced diastereoselectivities. In the amination direction, they catalyze the conversion of mesaconate to yield only (2*S*,3*S*)-3-methylaspartic acid, with no detectable formation of (2*S*,3*R*)-3-methylaspartic acid. The results are discussed in terms of a mechanism in which Lys331, His194, and Gln329 are involved in positioning the substrate and in formation and stabilization of the enolate anion intermediate.

Introduction

3-Methylaspartate ammonia-lyase (MAL) catalyzes the reversible amination of mesaconate (**1**) to give (2*S*,3*S*)-3-methylaspartic acid (**2**) as a major product and (2*S*,3*R*)-3-methylaspartic acid (**3**) as a minor product (Scheme 1).[1,2] The enzyme is used

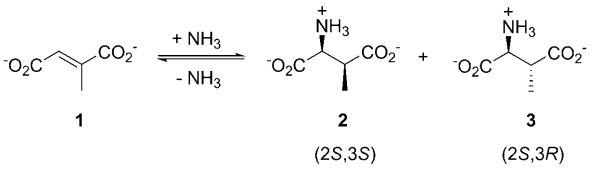

Scheme 1. MAL-catalyzed reversible amination of mesaconate to yield (2*S*,3*S*)- and (2*S*,3*R*)-3-methylaspartic acid.

by the anaerobic bacterium *Clostridium tetanomorphum* as part of a degradative pathway that converts (*S*)-glutamic acid via **2** to finally yield acetyl-CoA.[1,2] MAL is of considerable biocatalytic interest because it also catalyzes the stereo- and regioselective addition of ammonia to several derivatives of **1** to form a number of 3-alkyl- and 3-halo-substituted aspartic acids.[3] Moreover, the broad nucleophile specificity of MAL enables the use of a range of alternative nucleophiles such as methylamine, ethylamine, hydrazine, and methoxylamine in the conjugate addition reaction.[4] These properties make MAL a promising biocatalyst for the enantiospecific synthesis of both 3- and N-substituted aspartic acids, which are interesting building blocks for pharmaceutical synthesis.

MAL is a homodimeric enzyme (molecular mass of ~45.5 kDa) that requires both monovalent (i.e., K^+) and divalent (i.e., Mg^{II}) cations for activity.[1,2] Several studies have

[a] *H. Raj, V. Puthan Veetil, C. R. Reis, Prof. Dr. W. J. Quax, Dr. G. J. Poelarends*
Department of Pharmaceutical Biology
Groningen Research Institute of Pharmacy, University of Groningen
Antonius Deusinglaan 1, 9713 AV Groningen (The Netherlands)
Fax: (+31) 50-3633000
E-mail: g.j.poelarends@rug.nl

[b] *B. Weiner, Prof. Dr. B. L. Feringa*
Department of Organic and Molecular Inorganic Chemistry
Stratingh Institute for Chemistry, University of Groningen
Nijenborgh 4, 9747 AG Groningen (The Netherlands)

[c] *Prof. Dr. D. B. Janssen*
Department of Biochemistry, Groningen Biomolecular Sciences and Biotechnology Institute, University of Groningen
Nijenborgh 4, 9747 AG Groningen (The Netherlands)

Supporting information for this article is available on the WWW under http://dx.doi.org/10.1002/cbic.200900311.

been aimed at demonstrating the deamination mechanism of MAL.[5–11] Some of these have suggested that MAL operates through a carbanion mechanism with rate-limiting C–N bond cleavage.[5,6] This proposed mechanism is supported by the observation that C3 hydrogen exchange of the C3-deuterated substrate (**2**, Scheme 1) with solvent occurs more rapidly than C–N bond cleavage. Moreover, no primary isotope effect was observed for the deamination of the C3-deuterated substrate.[5,6] Nonetheless, other reports have questioned this carbanion mechanism,[7–11] and up until the structure of MAL was reported, the catalytic mechanism of the enzyme remained unresolved.

The crystal structure of MAL from *C. tetanomorphum*[12] and that of the isozyme from *Citrobacter amalonaticus*[13] were reported a few years ago. These structures showed that within the functional homodimer, each MAL monomer consists of two domains (Figure 1 A). The larger C-terminal domain is an eightfold α/β barrel, and the smaller N-terminal domain mainly consists of β strands. The active site carrying the essential Mg^{II} ion is located in a large cleft between the two domains. Structure comparisons identified MAL as a member of the enolase superfamily.[12,13] Despite little sequence identity, the overall α/β-barrel topology and the active-site architecture of MAL are strikingly similar to those of enolase, the title enzyme of this superfamily. Interestingly, the members of the enolase superfamily catalyze different reactions but share a common catalytic step: the metal-ion-assisted, general-base-catalyzed abstraction of the α proton of a carboxylic acid substrate to generate an enzyme-stabilized enolate anion intermediate.[14] On the basis of the structural homology to the enolase superfamily, coupled with the earlier results of kinetic isotope studies, it was proposed that MAL functions by using the common enolase catalytic step, and thus generates and stabilizes an enolate anion intermediate (**4**, Scheme 2).[12,13]

Although a general base catalyst for the deamination activity of MAL has not been determined, Lys331 appears to be a likely candidate because it occupies a similar position to the general base Lys345 in enolase.[12,13] Moreover, the crystal structure of *C. amalonaticus* MAL in complex with **2** shows that Lys331 is the only candidate in the vicinity of C3 that can function as a general base catalyst (Figure 1 B).[13] Two other residues, His194 and Gln329, are implicated in binding the C4 carboxylate group of **2** (Figure 1 B),[13] and thus are likely candidates for assisting the Mg^{II} ion in stabilizing the enolate anion intermediate. It was further postulated that His194 might also function as the second base (in addition to Lys331) that abstracts the C3 proton of the stereoisomer **3** (Scheme 1).[12]

The objective of the present work is twofold. First, we demonstrate the importance of His194, Gln329, and Lys331 for the MAL-catalyzed reactions. Second, we show that mutations of these active-site residues alter the diastereoselectivity of MAL. This led to a single amino acid MAL variant (H194A) that has useful properties for the stereoselective synthesis of isomerically pure (2*S*,3*S*)-3-methylaspartic acid. The results are discussed in terms of a mechanism in

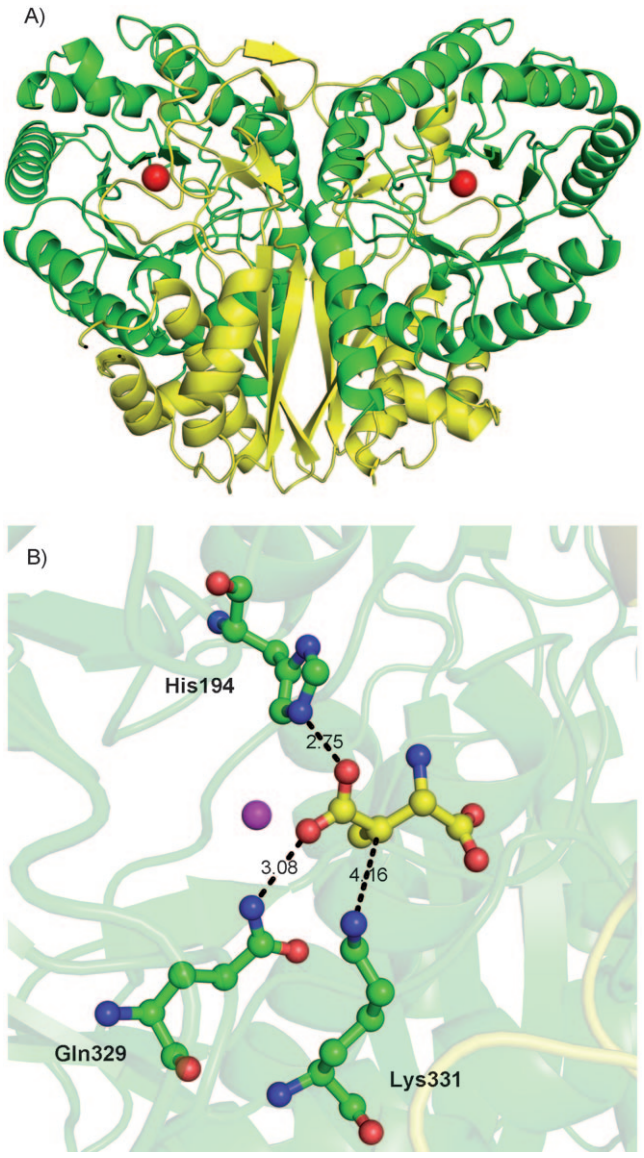

Figure 1. A) Ribbon diagram of the functional homodimeric structure of *C. amalonaticus* MAL.[13] The location of the active site in each monomer is indicated by the bound Mg^{II} ion, which is shown as a red sphere. The figure was prepared with PyMOL.[27] B) A close-up of the active site of *C. amalonaticus* MAL in complex with (2*S*,3*S*)-3-methylaspartic acid.[13] For clarity, only the Mg^{II} ion (magenta sphere) and the active-site residues His194, Gln329, and Lys331 are shown. The roles of these residues and their interactions are discussed in the text. Observed distances (in Å) between active site residues and substrate are indicated. The figure was prepared with PyMOL.[27]

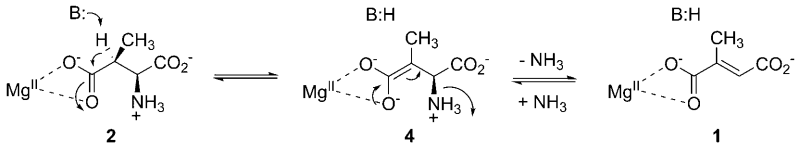

Scheme 2. Proposed enolate anion intermediate along the reaction pathway of MAL.

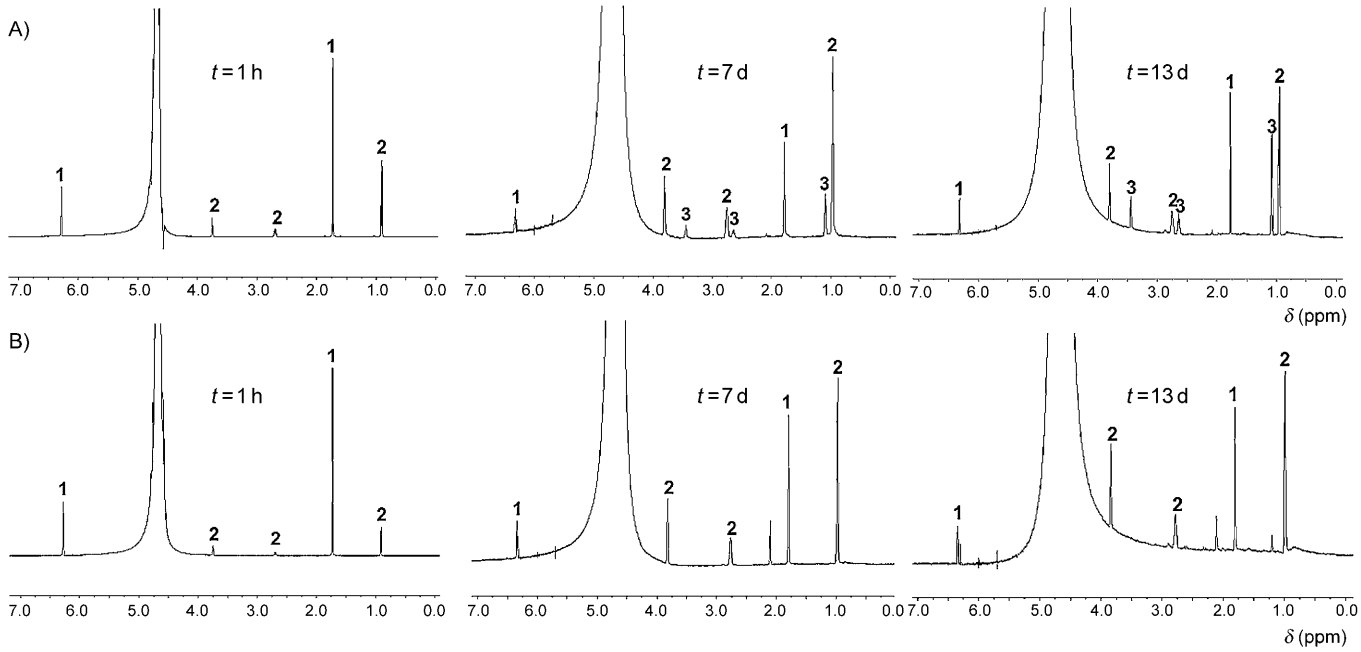

Figure 2. ^{1}H NMR spectra monitoring the amination of **1** by A) MAL and B) the H194A mutant. The ^{1}H NMR signals for compounds **1**, **2**, and **3** are indicated (see the Supporting Information for assignment of the signals). Spectra were recorded after 1 h, 7 d, and 13 d, as shown from left to right, respectively. The ^{1}H NMR spectra of the K331A and Q329A mutants (not shown) were comparable to those of the H194A mutant; that is, there was no detectable formation of **3** in the incubation mixtures. The less prominent singlets at δ1.20 and 2.11 ppm correspond to impurities resulting from multiple additions of protein.

which His194, Gln329, and Lys331 are involved in binding and positioning of the substrate, and in formation and stabilization of the enolate anion intermediate.

Results

Expression and purification of MAL

The gene coding for MAL was amplified from genomic DNA of *C. tetanomorphum* and fused into the start codon of the expression vector pBAD/*Myc*-His A, resulting in the construct pBAD(MAL-His). Sequencing of the cloned MAL gene verified that no mutations had been introduced during the amplification and cloning procedures. The MAL gene in pBAD(MAL-His) is under transcriptional control of the *araBAD* promoter and the recombinant enzyme was produced upon induction with arabinose in *E. coli* TOP10 as a C-terminal hexahistidine fusion protein. Production of soluble and active MAL was most efficient when cells were cultivated at 17 °C and when 0.004 % (*w*/*v*) arabinose was used. The recombinant enzyme was purified by a one-step Ni-based immobilized metal affinity chromatography protocol, which typically provides 10–15 mg of homogeneous enzyme per liter of culture.

Kinetic and ^{1}H NMR spectroscopic analysis of the MAL-catalyzed amination of 1

A mixture containing MAL, mesaconate (**1**), and ammonium chloride was monitored by ^{1}H NMR spectroscopy to verify that the products of the reaction are (2*S*,3*S*)-3-methylaspartic acid (**2**) and (2*S*,3*R*)-3-methylaspartic acid (**3**), as has been previously reported.[2] Indeed, the enzymatic amination of **1** yields **2** and **3**, as indicated by signals in the NMR spectra consistent with the structures of these amino acid products (Figure 2 A).[15] Although the ^{1}H NMR spectra showed signals for both **2** and **3**, those corresponding to **2** predominated in the initial spectra whereas signals for **3** appeared only in the later spectra. These observations confirm that MAL catalyzes the rapid conversion of **1** to the natural substrate **2**, as well as the slow conversion of **1** to **3**. After a 13-day incubation period, the MAL-catalyzed reaction was complete; the reaction resulted in 45 % **2** and 35 % **3**.

A previously described assay[3] was used to measure the kinetic parameters for MAL in the amination direction. Accordingly, the rate of amination of **1** was monitored by following the depletion of **1** at 270 nm in 500 mM Tris–HCl buffer (pH 9.0) containing 20 mM $MgCl_2$ and 400 mM NH_4Cl at 30 °C. A k_{cat} of $61 \pm 1\ s^{-1}$ and a K_M of 0.7 ± 0.02 mM were found; this results in a k_{cat}/K_M of $\sim 8.7 \times 10^4\ M^{-1} s^{-1}$ (Table 1).

Table 1. Apparent kinetic parameters for the MAL, K331A, H194A, and Q329A-catalyzed amination of mesaconic acid (**1**)[a]

Enzyme	k_{cat} [s^{-1}]	K_M (for **1**) [mM]	k_{cat}/K_M [$M^{-1} s^{-1}$]
MAL	61 ± 1	0.7 ± 0.02	8.7×10^4
K331A	n.d.	n.d.	< 0.001
H194A	8.4 ± 0.3	14 ± 1	6.0×10^2
Q329A	0.25 ± 0.02	1.7 ± 0.2	1.5×10^2

[a] The steady state kinetic parameters were determined in 500 mM Tris–HCl buffer (pH 9.0) containing 20 mM $MgCl_2$ and 400 mM NH_4Cl at 30 °C. Errors are standard deviations. n.d., not determined.

Kinetic and ^{1}H NMR spectroscopic analysis of the MAL-catalyzed deamination of 2

The rate of deamination of **2** by MAL was monitored by following the formation of **1** at 240 nm in 500 mM Tris–HCl buffer (pH 9.0) containing 20 mM $MgCl_2$ and 1 mM KCl at 30 °C.[3] For the deamination of **2**, a k_{cat} of $89 \pm 4\ s^{-1}$ and a K_M of 1.0 ± 0.1 mM were found; this results in a k_{cat}/K_M of $8.9 \times 10^4\ M^{-1}s^{-1}$ (Table 2).

Table 2. Kinetic parameters for the MAL, K331A, H194A, and Q329A-catalyzed deamination of (2*S*,3*S*)-3-methylaspartic acid (**2**)[a]

Enzyme	k_{cat} [s^{-1}]	K_M [mM]	k_{cat}/K_M [$M^{-1}s^{-1}$]
MAL	89 ± 4	1.0 ± 0.1	8.9×10^4
K331A	n.d.	n.d.	< 0.001
H194A	0.55 ± 0.01	1.8 ± 0.2	3.1×10^2
Q329A	0.01 ± 0.001	1.0 ± 0.1	1.0×10^1

[a] The steady state kinetic parameters were determined in 500 mM Tris–HCl buffer (pH 9.0) containing 20 mM $MgCl_2$ and 1 mM KCl at 30 °C. Errors are standard deviations. n.d., not determined.

A mixture containing MAL and **2** was also monitored by ^{1}H NMR spectroscopy to verify that the product of the reaction is **1**. The enzymatic conversion of **2** yields **1**, as indicated by a singlet at 1.74 ppm and a singlet at 6.28 ppm (Figure S4 in the Supporting Information), which correspond to the protons at the C3 methyl group and C2, respectively. In addition, signals corresponding to **3** are also present. After a 13-day incubation period, the MAL-catalyzed reaction results in 41% **1** and 2% **3**.[16] Hence, **1** is the major product of the MAL-catalyzed conversion of **2**.

^{1}H NMR spectroscopic analysis of the MAL-catalyzed deamination of 3

^{1}H NMR spectroscopic analysis of the diastereoisomer **3** revealed that the provided material contained 94–95% of the required diastereoisomer **3** and 5–6% of the unwanted diastereoisomer **2**. This finding precluded the use of the material in kinetic experiments. Nevertheless, it was possible to monitor the deamination of **3** by ^{1}H NMR spectroscopy and identify the products of the reaction. The ^{1}H NMR spectra showed the disappearance of signals corresponding to **3** and the appearance of new signals corresponding to **1** and **2**. Signals corresponding to **1** predominated in the initial spectra whereas signals for **2** increased in the later spectra. After a lengthy incubation period (approximately two weeks), the MAL-catalyzed reaction was complete; it yielded **1** in 79% and **2** in 12% (Figure S5).

Mutagenesis of His194, Lys331, and Gln329

To investigate the importance of His194, Lys331, and Gln329 for the activity and stereoselectivity of MAL, single site-directed mutants were constructed in which His194 and Gln329 were replaced with either an alanine or arginine (H194A, H194R, Q329A, and Q329R) and Lys331 with a glycine, alanine, glutamine, histidine, or arginine (K331G, K331A, K331Q, K331H, and K331R). DNA sequencing verified that only the intended mutations had been introduced into each mutant gene. The mutants were overexpressed in *E. coli* strain TOP10 and purified to >95% homogeneity (as assessed by SDS-PAGE) by using the Ni-based immobilized metal affinity chromatography protocol described for wild-type MAL. The yields (in milligrams of homogeneous protein per liter of cell culture) of the mutants varied from 10 to 20 mg.

It was shown by nondenaturing PAGE (data not shown) that the native molecular mass for each mutant is comparable to that of wild type; this demonstrates that the oligomeric association of the mutants was still intact. The structural integrity of the mutants was also assessed by circular dichroism (CD). The CD spectra of the mutants were comparable to that of the wild type; this indicates that these mutations did not result in any major conformational changes (Figure S6).

Kinetic and ^{1}H NMR spectroscopic analysis of the deamination of 2 by the MAL mutants

The activities of the MAL mutants were initially assayed by using the natural substrate **2**. It was found that substitution of Lys331 by a glycine, alanine, histidine, glutamine, or arginine essentially abolished enzymatic activity, and this underscores the importance of this residue for the MAL-catalyzed deamination of **2**. Under the conditions of the kinetic assays, no activity could be detected for these mutants. Substitution of either His194 or Gln329 by an arginine also resulted in mutant enzymes that were inactive. The H194A and Q329A mutants, however, deaminate **2** at a reduced catalytic efficiency (Table 2). For the H194A mutant, there is a slight (1.8-fold) increase in K_M and a ~160-fold decrease in k_{cat}; this results in a ~290-fold reduction in k_{cat}/K_M. For the Q329A mutant, there is a ~8900-fold decrease in k_{cat}, whereas the K_M is not affected. Hence, this results in a ~8900-fold reduction in k_{cat}/K_M.

The deamination activities of the three alanine mutants (H194A, K331A, and Q329A) were also assessed by ^{1}H NMR spectroscopy after a lengthy (approximately two weeks) incubation period. With **2**, the H194A and Q329A-catalyzed reactions resulted in a 40% yield of **1** and a 3% yield of **3**, whereas the K331A-catalyzed reaction showed only a trace amount of product (2% **1** and 2% **3**).[16] These observations parallel those of the kinetic assays and suggest that Lys331 is more critical for the deamination activity of MAL than His194 and Gln329.

pH dependence of the kinetic parameters of MAL and the H194A mutant by using 2

To determine the pK_a of the basic group on the enzyme important for catalysis (the presumed general base catalyst) and to evaluate the effect of the alanine mutation on this pK_a, the pH dependence of the k_{cat}/K_M for the MAL and H194A-catalyzed deamination of **2** was determined over the pH range 6.0–9.5. The other two alanine mutants, K331A and Q329A, were not active enough with **2** and thus could not be measured. The

log (k_{cat}/K_M) versus pH profiles of MAL and H194A both show a single ascending limb with a slope of one (Figure 3).[17] For wild-type MAL, a pK_a value of 7.8 ± 0.1 was found. For the H194A mutant, a pK_a value of 8.2 ± 0.1 was found. Hence, within the estimated errors, there is no significant effect of the H194A substitution on the pK_a for the ascending limb.

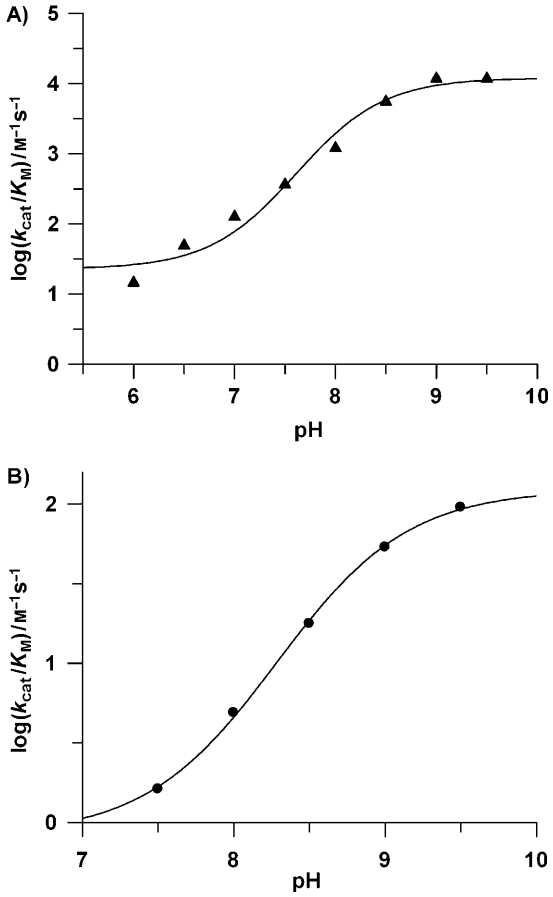

Figure 3. The pH dependence of log(k_{cat}/K_M) for the deamination of **2** by A) wild-type MAL and B) the H194A mutant. The pK_a values are discussed in the text.

^{1}H NMR spectroscopic analysis of the K331A, H194A, and Q329A-catalyzed deamination of 3

The deamination of the nonnatural substrate **3** by the alanine mutants was monitored by ^{1}H NMR spectroscopy. After a 13 day-incubation period, the Q329A-catalyzed reaction resulted in a 10% yield of **1**. The contaminant **2**, which is the natural substrate for the enzyme, was selectively processed by Q329A at a much faster rate than for **3**. The H194A mutant also processed the contaminant **2** (this resulted in a 6% yield of **1**), but showed no detectable activity towards **3**. The mixture containing the K331A mutant showed no product.

Kinetic and ^{1}H NMR spectroscopic analysis of the amination of 1 by the MAL mutants

The kinetic parameters for the amination reactions catalyzed by the MAL mutants were determined and compared to those measured for the wild-type MAL-catalyzed amination of **1** (Table 1). For the Q329A mutant, there is a slight increase in K_M (~2.4-fold) and a ~240-fold decrease in k_{cat}, which results in a ~600-fold reduction in k_{cat}/K_M. For the H194A mutant, there is a 20-fold increase in K_M and only about a sevenfold decrease in k_{cat}, which results in a ~140-fold reduction in k_{cat}/K_M. Under the conditions of the kinetic assay, no activity could be detected for the other mutants (H194R, Q329R, K331G, K331A, K331Q, K331H, and K331R).

The amination of **1** by the three alanine mutants (H194A, Q329A, and K331A) was also monitored by ^{1}H NMR spectroscopy to identify the diastereoisomeric products of the reaction. After a 13-day incubation period, the K331A, Q329A, and H194A-catalyzed reactions resulted in 30%, 58%, and 85% diastereoisomer **2**, respectively (Figure 2B; data not shown). Interestingly, and in contrast to the wild-type MAL-catalyzed amination of **1** (Figure 2A), there was no detectable formation of diastereoisomer **3** in the incubation mixtures. For comparison, conversion of 35% of **1** by wild-type MAL results in a 19% yield of **2** and 16% of **3**. These observations indicate that the H194A, Q329A, and K331A mutants have enhanced diastereoselectivities and catalyze the highly stereoselective conversion of **1** to **2**, with no detectable conversion of **1** to **3**.

Discussion

Previous studies of the stereoselectivity of *C. tetanomorphum* MAL indicated that the wild-type enzyme catalyzes the reversible *anti* and *syn*-addition of ammonia to mesaconate (**1**) to yield (2*S*,3*S*)-3-methylaspartic acid (**2**) and (2*S*,3*R*)-3-methylaspartic acid (**3**), respectively.[2,9] The determination of the X-ray structure of *C. amalonaticus* MAL in complex with the natural substrate **2** has provided the essential structural information for the identification of the substrate interactions within the enzyme–substrate complex.[13] Guided by the structure of this complex, we have selected three active site residues in *C. tetanomorphum* MAL[12] for mutagenesis to provide insight into the structural determinants of the reactivity and stereoselectivity of MAL.[18] The results of these studies are interpreted here and discussed in terms of a two-base mechanism, in which the proton abstraction/addition steps are effected by *S* and *R*-specific general base/acid catalysts juxtaposed on either side of the (chiral) C3 carbon of the substrate.

We first verified that both **2** and **3** are formed as products of the MAL-catalyzed amination of **1** by ^{1}H NMR spectroscopy. It was found that stereoisomer **2** is formed at a rate much faster than stereoisomer **3** (at equilibrium, the ratio of **2**/**3** is approximately 1.3). Second, we confirmed that MAL does not catalyze the direct epimerization of the two stereoisomers. This was evident from a prolonged incubation of MAL with **2**; this yielded **1** as the major product and gave only a trace amount of **3**. Another notable observation is that the incubation of MAL with **3**

finally gives **2** (in 12% yield), but only after a significant amount of **1** accumulates in the reaction mixture. This suggests that MAL first catalyzes the *syn*-elimination of ammonia from **3** to yield **1**, and this is followed by the *anti*-addition of ammonia to **1** to give **2**. These observations indicate that the formation of **2** and **3** as products of the MAL-catalyzed amination of **1** is not the result of the MAL-catalyzed amination of **1** to **2** followed by the slow direct epimerization of **2** to **3**. Hence, MAL indeed catalyzes the rapid *anti*-addition and the much slower *syn*-addition of ammonia to **1** to give **2** and **3**, respectively.

The crystal structure of *C. amalonaticus* MAL in complex with **2** shows that Lys331 is the only candidate in the vicinity of C3 that can function as the *S*-specific base/acid catalyst (Figure 1 B).[13] This lysine residue is conserved in all characterized 3-methylaspartate ammonia-lyases. Moreover, a comparison of the active-site structures of MAL and enolase shows that Lys331 in MAL superimposes to within 1 Å of the previously identified general base Lys345 in enolase.[13] To assess its role in catalysis, we have mutated Lys331 to a glycine, alanine, histidine, glutamine, or arginine. Examination of the kinetic properties for these mutants clearly shows that Lys331 is an essential residue in the MAL-catalyzed reactions because all five mutations at this position result in a dramatic loss of activity. (There is a $>10^7$-fold drop in the value of k_{cat}/K_M with **2**). The mutant enzymes appear to retain an intact overall structural integrity as shown by CD spectroscopy. It is therefore reasonable to conclude that Lys331 is crucial for catalysis because it functions as the *S*-specific base catalyst in the deamination of **2** and, hence, as the acid catalyst (the conjugate acid of Lys331) in the corresponding reverse *anti*-addition reaction (Scheme 3).

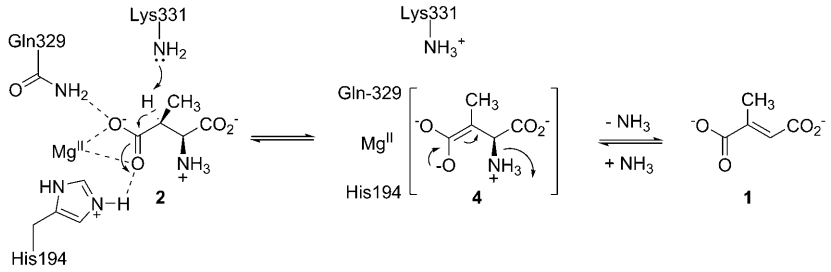

Scheme 3. A schematic representation of the proposed catalytic mechanism of MAL, showing the key participants in the deamination of (2*S*,3*S*)-3-methylaspartic acid.

From the ascending limb of the log (k_{cat}/K_M) versus pH profile of MAL, a residue with a pK_a of approximately 7.8 that must be deprotonated for optimal activity, might be the general base catalyst involved in abstraction of the C3 proton of **2**. Whereas the pK_a value of Lys331 in MAL has not been directly measured by NMR spectroscopy, it can be inferred from these results that the kinetic pK_a value of 7.8 is likely due to Lys331.

In the structure of the MAL-substrate complex, His194 and Gln329 are hydrogen bonded to the C4 carboxylate group of **2** (Figure 1 B).[13] This suggests roles for these residues in binding the substrate, and possible intermediates, in the reaction mechanism of MAL. In this study, His194 and Gln329 were mutated to assess their role in catalysis. The best-characterized mutants are the H194A and Q329A mutants, which have measurable activity and show no significant differences in their CD spectra compared to that of wild-type MAL. Examination of the kinetic properties for the two mutants in the deamination direction (by using **2**) shows that there is a small effect on K_M and a much larger effect on k_{cat}. This suggests important roles for His194 and Gln329 in catalysis. The somewhat larger effect of these mutations on the value of K_M in the amination direction might suggest a more important role for His194 and Gln329 in binding **1** than **2**.

A major part of the loss in activity of the H194A and Q329A mutants is likely due to the removal of optimal hydrogen-bonding interactions with the proposed enolate anion intermediate formed at the C4 carbonyl position of **2** (or **1** in the corresponding reverse reaction); this makes the abstraction of a proton from the C3 position less favorable. Presumably, His194 and Gln329, together with the essential Mg^{II} ion, polarize the C4 carboxylate group and stabilize the enolate anion

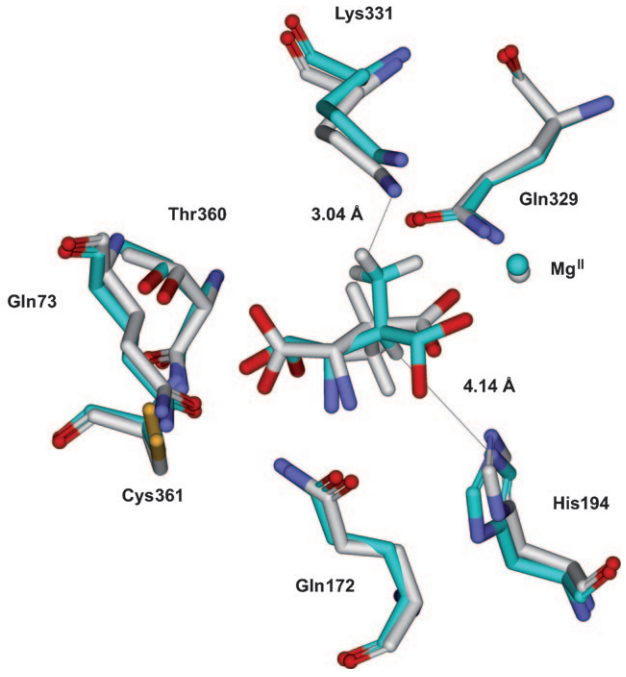

Figure 4. Close-up view of two superimposed active sites of *C. amalonaticus* MAL, one in complex with the natural substrate (2*S*,3*S*)-3-methylaspartic acid (**2**)[13] (shown in gray) and the other with the most-favored conformation of the modeled nonnatural substrate (2*S*,3*R*)-3-methylaspartic acid (**3**) (shown in cyan). The orientation of **2** suggests that its C3 proton is abstracted by Lys331, whereas the orientation of **3** suggests that its C3 proton is abstracted by His194. The figure was prepared with Discovery Studio 1.7.

intermediate **4** that is formed upon abstraction of the C3 proton (Scheme 3). An electrophilic residue, the role of which is to assist the Mg^{II} ion in providing the charge neutralization that is essential for the activation of the α proton and for stabilizing the enolate anion intermediate, has also been identified in mandelate racemase (Lys164) and some other enolase superfamily members.[14,19]

In addition to its presumed role as electrophilic residue, His194 might also function as the *R*-specific base/acid catalyst. Naismith and co-workers first proposed this role for His194 based on structure comparisons of enolase superfamily members.[12] The sidechain of His194 superimposes on that of the second base Lys166 in mandelate racemase and the principal base Lys213 in glucarate dehydratase.[12] Moreover, if the three-dimensional structure of **3** is modeled into the active site of MAL by using the X-ray structure of MAL in complex with **2** as a guide, then the C3 proton of **3** is faced towards the imidazole nitrogen atom (Nε2) of His194 (Figure 4). Our experiments clearly show that His194 is an important determinant of the stereoselectivity of MAL because an alanine mutation at this position results in a mutant enzyme that appears to have lost its ability to catalyze proton abstraction/addition from the *R* face (the His194 side) of the substrate. Indeed, the H194A mutant has no detectable deamination activity with **3** and catalyzes the highly stereoselective conversion of **1** to **2**, with no detectable formation of **3**. Taken together, these observations are consistent with a role of His194 as the *R*-specific general base catalyst for the deamination of **3** and, hence, as the acid catalyst (the conjugate acid of His194) in the corresponding reverse *syn*-addition reaction.

In view of the presumed role of His194 as the *R*-specific general base/acid catalyst, mutation of Lys331 or Gln329 to an alanine gave results that were somewhat unexpected. Initially, it was thought that mutation of Lys331 would only effect proton abstraction/addition from the *S* face (the Lys331 side) of the substrate. Surprisingly, however, the K331A mutant lost its ability to catalyze proton abstraction/addition from the *R* face of the substrate, but it retained a very low-level proton abstraction/addition activity from the *S* face of the substrate. Like K331A, the Q329A mutant also catalyzes the highly stereoselective conversion of **1** to **2** with no detectable formation of **3**. But, in contrast to K331A, the Q329A mutant still has a detectable low-level deamination activity with **3**.

One potential explanation for the alteration in diastereoselectivity of the K331A and Q329A mutants is that mutation of Lys331 or Gln329 to an alanine causes different interactions between substrate and enzyme and might influence the geometry of a Michaelis complex that undergoes proton abstraction/addition from the *R* face of the substrate. In this scenario, the removal of the native interactions with the substrate places the substrate in an unfavorable position to undergo proton abstraction/addition by His194, the presumed *R*-specific base/acid catalyst. Another explanation for the loss in proton abstraction/addition activity from the *R* face of the substrate is that mutation of Lys331 or Gln329 by an alanine directly influences the orientation of the His194 sidechain. Crystallographic studies of the H194A, K331A, and Q329A mutants, and of wild-type MAL in complex with **3**, would be an important step toward understanding how these mutations affect the stereochemical properties of MAL.

The current investigation has clearly demonstrated that the stereoselectivity of MAL can be enhanced by mutation of the active-site residues His194, Lys331, and Gln329. Interestingly, the mutation of Gln73 or Gln172, two residues implicated in binding the C2 amino group of **2** (Figure 4), to an alanine has a profound effect on the values of k_{cat} and k_{cat}/K_M (with **1** and **2**) but no significant effect on the stereoselectivity of MAL. Like wild-type MAL, the Q73A and Q172A mutants catalyze the amination of **1** to give both **2** and **3** as products (H.R., G.J.P., unpublished results, **2009**). Hence, His194, Gln329, and Lys331 appear to be the major determinants of the stereoselectivity of MAL. The enhancement of the stereoselectivity should make it possible to utilize single amino acid variants of MAL (e.g., H194A) in stereo- and regioselective amination reactions to produce 3-substituted aspartic acid isomers with a very high diastereomeric excess. Such efforts are being pursued in our laboratories.

Experimental Section

Materials: DL-*threo*-3-methylaspartic acid, mesaconic acid, and L-arabinose were purchased from Sigma–Aldrich. (2*S*,3*R*)-3-Methylaspartic acid (95% purity) was purchased from Syncom (Groningen, The Netherlands). Ingredients for buffers and media were obtained from Duchefa Biochemie (Haarlem, The Netherlands) or Merck. Molecular biology reagents, including restriction enzymes, PCR reagents, T4 DNA ligase, DNA ladders, agarose, and protein molecular weight standards were obtained from F. Hoffmann–LaRoche, Promega, Invitrogen, Finnzymes (Espoo, Finland) or New England Biolabs. PCR purification, gel extraction, and Miniprep kits were provided by Macherey–Nagel (Düren, Germany). Pre-packed PD-10 Sephadex G-25 columns were purchased from GE Healthcare Bio-Sciences. Oligonucleotides for DNA amplification were synthesized by Operon Biotechnologies (Cologne, Germany).

Bacterial strains, plasmids, and growth conditions: *E. coli* strain XL1-Blue (Stratagene, La Jolla, CA) was used for cloning and isolation of plasmids. *E. coli* strain TOP10 (Invitrogen) was used in combination with the pBAD/*Myc*-His A vector (Invitrogen) for recombinant protein production. *C. tetanomorphum* ATCC 15920, the genomic DNA source for the MAL gene, was purchased from DSMZ GmbH (Braunschweig, Germany). *E. coli* cells were grown in Luria–Bertani (LB) media. When required, Difco agar (15 g/L), ampicillin (Ap, 100 μg mL^{-1}), and/or arabinose (0.004% *w*/*v*) were added to the medium.

General methods: Techniques for restriction enzyme digestions, ligation, transformation, and other standard molecular biology manipulations were based on methods described elsewhere[20] or as suggested by the manufacturer. The PCR was carried out in a DNA thermal cycler (model GS-1) obtained from Biolegio (Nijmegen, The Netherlands). DNA sequencing was performed by ServiceXS (Leiden, The Netherlands) or Macrogen (Seoul, Korea). Protein was analyzed by PAGE under either denaturing conditions by using SDS or native conditions on gels containing polyacrylamide (7.5–10%). The gels were stained with Coomassie brilliant blue. Protein concentrations were determined by the Waddell method.[21] Kinetic data were obtained on a V-650 spectrophotometer from Jasco (IJsselstein, The Netherlands). The solutions in the cuvettes were

mixed by using a stir/add cuvette mixer (Bel-Art Products, Pequannock, NJ, USA). The kinetic data were fitted by nonlinear regression data analysis by using the Grafit program (Erithacus, Software Ltd., Horley, UK) obtained from Sigma Chemical Co. The CD spectra were recorded on a model 62A-DS spectropolarimeter from AVIV Biomedical Inc. (Lakewood, NJ, USA). ^{1}H NMR spectra were recorded on a Varian Inova 500 (500 MHz) spectrometer by using a pulse sequence for selective presaturation of the water signal. Chemical shifts for protons are reported in parts per million scale (δ scale) downfield from tetramethylsilane and are referenced to protium (H_2O: $\delta = 4.67$).

Construction of the expression vector for the production of MAL: The MAL gene was amplified by PCR by using two synthetic primers, a small amount of biomass from *C. tetanomorphum* as the genomic DNA source, and the PCR reagents supplied in the Expand High Fidelity PCR system by following the protocol supplied with the system (F. Hoffmann-La Roche, Ltd.). The forward primer (5′-ATA **CAT ATG** AAA ATT GTT GAC GTA CTT TG-3′) contains a NdeI restriction site (in bold) followed by 20 bases corresponding to the coding sequence of the MAL gene. The reverse primer (5′-CAT **AAG CTT** TTT TCT TCT TCC TAC AAG-3′) contains a HindIII restriction site (in bold) followed by 18 bases corresponding to the complementary sequence of the MAL gene. The resulting PCR product and the pBAD*N*/*Myc*-His A vector were digested with NdeI and HindIII restriction enzymes, purified, and ligated by using T4 DNA ligase. The pBAD*N*/*Myc*-His A vector is a variant of the commercially available pBAD/*Myc*-His A vector in which the unique NcoI site is replaced with NdeI.[22] Aliquots of the ligation mixture were transformed into competent *E. coli* TOP10 cells. Transformants were selected at 37 °C on LB/Ap plates. Plasmid DNA was isolated from several colonies and analyzed by restriction analysis for the presence of the insert. The cloned MAL gene was sequenced to verify that no mutations had been introduced during the amplification of the gene. The newly constructed expression vector was named pBAD(MAL-His).

Construction of MAL mutants: Mutants of MAL were generated by the overlap extension PCR method[23] by using plasmid pBAD-(MAL-His) as the template. The final PCR products were gel purified, digested with the NdeI and HindIII restriction enzymes, and ligated in-frame with both the initiation ATG start codon and the sequence that codes for the polyhistidine region of the expression vector pBAD*N*/*Myc*-His A. All mutant genes were completely sequenced (with overlapping reads) to verify that only the intended mutation had been introduced.

Expression and purification of MAL wild type and mutants: The MAL enzyme, either wild type or mutant, was produced in *E. coli* TOP10 by using the pBAD expression system. Fresh TOP10 cells containing the appropriate expression plasmid were collected from a LB/Ap plate by using a sterile loop and used to inoculate LB/Ap medium (15 mL). After growth for 8 h at 37 °C, a sufficient quantity of the culture was used to inoculate fresh LB/Ap medium (300 mL) containing arabinose (0.004%, *w*/*v*) in a 1 L Erlenmeyer flask to an initial A_{600} of ~0.1. Cultures were grown for 4 d at 17 °C with vigorous shaking. Cells were harvested by centrifugation (6000 *g*, 15 min) and stored at −20 °C until further use.

In a typical purification experiment, cells (of three 300 mL cultures) were thawed, combined, and suspended in lysis buffer (10 mL, 50 mM NaH_2PO_4, 300 mM NaCl, 10 mM imidazole, pH 8.0). Cells were disrupted by sonication for 4×1 min (with 4–6 min rest in between each cycle) at a 60 W output, after which unbroken cells and debris were removed by centrifugation (10000 *g*, 45 min). The supernatant was filtered through a 0.45 μM pore diameter filter and incubated with Ni-NTA (1 mL slurry in a small column at 4 °C for ≥18 h), which had previously been equilibrated with lysis buffer. The nonbound proteins were eluted from the column by gravity flow. The column was first washed with lysis buffer (10 mL) and then with buffer A (50 mM NaH_2PO_4, 300 mM NaCl, 20 mM imidazole, pH 8.0; 10 mL). Retained proteins were eluted with buffer B (50 mM NaH_2PO_4, 300 mM NaCl, 250 mM imidazole, pH 8.0; 2.0 mL). Fractions (~0.5 mL) were analyzed by SDS-PAGE on gels containing acrylamide (10%), and those that contained purified MAL were combined and the buffer was exchanged against Tris buffer (50 mM, pH 8.0), containing $MgCl_2$ (2 mM) and KCl (0.1 mM), by using a prepacked PD-10 Sephadex G-25 gel filtration column. The purified enzyme was stored at +4 °C or −80 °C until further use.

Circular dichroism spectroscopy: Circular dichroism spectra of the wild-type protein and the purified mutants were measured in Tris–HCl buffer (10 mM, pH 8.0), containing $MgCl_2$ (2 mM) and KCl (0.1 mM), at a concentration of approximately 3.2 μM in a CD cell with a 1.0 mm optical path length.

Kinetic assays: The assays used for the spectrophotometric determination of the deamination of **2** and to follow the amination of **1** are based on protocols reported elsewhere.[3] Accordingly, the deamination of **2** by MAL was monitored by following the formation of **1** at 240 nm ($\varepsilon = 3850\ M^{-1}cm^{-1}$) in Tris–HCl buffer (500 mM, pH 9.0) containing $MgCl_2$ (20 mM) and KCl (1 mM) at 30 °C. An aliquot of MAL, either wild type or mutant, was diluted into buffer (20 mL) and incubated for 30 min at 30 °C. The 30 min equilibration period resulted in more reproducible kinetic data. Subsequently, a portion (1 mL) was transferred to a 10 mm quartz cuvette and the enzyme activity was assayed by the addition of a small quantity (1–10 μL) of **2** from a stock solution. The stock solutions were made up by dissolving the appropriate amount of DL-*threo*-3-methylaspartic acid (a 1:1 mixture of the enantiomers (2*S*,3*S*)-3-methylaspartic acid and (2*R*,3*R*)-3-methylaspartic acid) in Tris–HCl buffer (500 mM, pH 9.0) to obtain the desired concentration of **2**. The (2*R*,3*R*)-enantiomer is neither a substrate nor an inhibitor of MAL. The concentrations of **2** that were used in the assay ranged from 0.5 to 20 mM.

The rate of amination of **1** was monitored by following the depletion of **1** at 270 nm ($\varepsilon = 482\ M^{-1}cm^{-1}$) in Tris–HCl buffer (500 mM, pH 9.0) containing $MgCl_2$ (20 mM) and NH_4Cl (400 mM) at 30 °C.[3] An aliquot of MAL, either wild-type or mutant, was diluted into buffer (20 mL) and incubated for 30 min at 30 °C. Subsequently, a portion (1 mL) was transferred to a 1 or 10 mm quartz cuvette and the enzyme activity was assayed by the addition of a small quantity (1–10 μL) of **1** from a stock solution. The stock solutions were made up in Tris–HCl buffer (500 mM, pH 9.0). The concentrations of **1** that were used in the assay ranged from 0.1 to 50 mM.

pH dependence of the kinetic parameters of MAL and H194A: The pH dependence of the steady-state kinetic parameters was determined in Tris buffer (500 mM) containing $MgCl_2$ (20 mM) and KCl (1 mM) with pH values ranging from 6.0–9.5. For each pH value, a sufficient quantity of enzyme (from a stock solution in Tris buffer (50 mM, pH 8.0) containing 2 mM $MgCl_2$ and 0.1 mM KCl) was equilibrated in buffer (20 mL) for 30 min at 30 °C. The addition of enzyme did not significantly change the pH. Subsequently, aliquots (1 mL) were removed and assayed for activity by using concentrations of **2** ranging from 0.5–50 mM. Stock solutions of **2** were made in Tris buffer (500 mM). The pH of the stock solutions was adjusted to each desired pH value (6.0–9.5). The volume of substrate added was 20 μL or less in all experiments.

^{1}H NMR spectroscopic product analysis of the amination of 1 by MAL wild type and mutants: The products of the amination of **1** by wild-type MAL and the MAL mutants were identified by ^{1}H NMR spectroscopy by using a procedure described elsewhere[2] with the following modifications. In separate experiments, MAL, K331A, H194A, or Q329A was incubated with **1**, and the reactions were followed by ^{1}H NMR spectroscopy. Reaction mixtures consisted of Na_2HPO_4 buffer (350 μL; 100 mM, containing 20 mM $MgCl_2$ and 1 mM KCl, pH 9.0), D_2O (50 μL), NH_4Cl (100 μL, 5 M), and an aliquot of **1** (100 μL) from a 500 mM stock solution. The stock solution of **1** was made in Na_2HPO_4 buffer (100 mM), and the pH of the solution was adjusted to 9.0 with aliquots of an aq 1 M NaOH solution. A quantity of enzyme (50 μL) was added from a stock solution and the reaction mixtures were incubated at 22 °C. The concentrations of the protein stock solutions were MAL (12.3 mg mL^{-1}), K331A (13.4 mg mL^{-1}), H194A (10.7 mg mL^{-1}), and Q329A (14.4 mg mL^{-1}). Additional aliquots of enzyme (50 μL) were added to the individual mixtures after 3, 6, 9, and 12 days. ^{1}H NMR spectra were recorded 1 h, 3 d, 7 d, and 13 d after the first addition of enzyme. Product amounts were estimated by integration of the signals corresponding to **2** and **3**, if present. The ^{1}H NMR signals for **1**, **2**, and **3** are given in the Supporting Information (Figures S1, S2 and S3).

^{1}H NMR spectroscopic product analysis of the reaction of wild-type and mutant MAL with 2 or 3: The products of the deamination of **2** or **3** by wild-type MAL and the MAL mutants were identified by ^{1}H NMR spectroscopy. In separate experiments, MAL, K331A, H194A or Q329A was incubated with **2** or **3**. Reaction mixtures consisted of Na_2HPO_4 buffer (400 μL; 100 mM, containing 20 mM $MgCl_2$ and 1 mM KCl, pH 9.0), D_2O (40 μL), and an aliquot of **2** or **3** (150 μL) from a 500 mM stock solution. The stock solutions of **2** and **3** were made in Na_2HPO_4 buffer (100 mM), and the pH of the solutions was adjusted to 9.0 with aliquots of a 1 M aq NaOH solution. A quantity of enzyme (50 μL) was added from a stock solution and the reaction mixtures were incubated at 22 °C. The concentrations of the protein stock solutions were MAL (15.7 mg mL^{-1}), K331A (12.8 mg mL^{-1}), H194A (7.4 mg mL^{-1}), and Q329A (8.8 mg mL^{-1}). Additional aliquots of enzyme (50 μL) were added to the individual mixtures after 3, 6, 9, and 12 d. The eight reaction mixtures were examined by ^{1}H NMR spectroscopy after a 13-day incubation period, and the product amounts were estimated by integration of the signals corresponding to **1, 2** and **3**, if present.

Molecular docking: Comparative docking simulations were performed by using Discovery Studio 1.7 (Accelrys, San Diego, CA, USA). Models for the enzymes were based on the structures of *C. amalonaticus* MAL in complex with **2**[13] and *C. tetanomorphum* MAL in the absence of a bound ligand[12] (PDB IDs: 1KKR and 1KCZ, respectively). Hydrogen atoms were added automatically. Models of the substrates were constructed, and the energy was minimized by using the CHARMm force field.[24] Minimization was done by using a dielectric constant of one and a nonbonded cutoff distance of 12 Å. The substrates were docked by using the grid-based approach CDOCKER, a molecular dynamics (MD) simulated-annealing-based algorithm,[25,26] by using the experimentally determined binding site for **2** in *C. amalonaticus* MAL as coordinates. Initially, the enzyme active site was fixed, and the atoms of the substrate, either **2** or **3**, were allowed to move. For subsequent rounds of minimization, the constraints on the amino acids forming the active site were removed and replaced by distance constraints based on the reported distances observed in X-ray structure of MAL complexed with **2**. A final minimization step was applied to each ligand-docked pose that consisted of 300 steps of steepest descent followed by 2500 iterations of the adopted basis-set Newton–Raphson algorithm with an energy tolerance of 0.001 Kcal mol^{-1}.

Abbreviations: Ap, ampicillin; CD, circular dichroism; LB, Luria–Bertani; MAL, 3-methylaspartate ammonia-lyase.

Acknowledgements

We gratefully acknowledge Gea K. Schuurman-Wolters (Department of Biochemistry, University of Groningen) for her assistance in acquiring the CD spectra. We are also grateful to Pieter van der Meulen (Molecular Dynamics group, University of Groningen) for his assistance in acquiring the NMR spectra. We thank Dr. Stefaan de Wildeman, Dr. Oliver May, Dr. Friso van Assema, and Dr. Bernard Kaptein (DSM Geleen, The Netherlands) for insightful discussions. This research was financially supported by the Netherlands Ministry of Economic Affairs and the B-Basic partner organizations (http://www.b-basic.nl) through B-Basic, a public-private NWO-ACTS programme. G.J.P. was supported by VENI and VIDI grants from the Division of Chemical Sciences of the Netherlands Organisation of Scientific Research (NWO-CW).

Keywords: amino acids · ammonia lyases · mutagenesis · protein engineering · stereoselectivity

[1] H. A. Barker, R. D. Smyth, R. M. Wilson, H. Weissbach, *J. Biol. Chem.* **1959**, *234*, 320–328.
[2] S. K. Goda, N. P. Minton, N. P. Botting, D. Gani, *Biochemistry* **1992**, *31*, 10747–10756.
[3] N. P. Botting, M. Akhtar, M. A. Cohen, D. Gani, *Biochemistry* **1988**, *27*, 2953–2955.
[4] M. S. Gulzar, M. Akhtar, D. Gani, *J. Chem. Soc., Perkin Trans. 1* **1997**, 649–655.
[5] H. J. Bright, *J. Biol. Chem.* **1964**, *239*, 2307–2315.
[6] H. J. Bright, L. L. Ingraham, R. E. Lundin, *Biochim. Biophys. Acta Spec. Sect. Enzymol. Subj.* **1964**, *81*, 576.
[7] N. P. Botting, M. A. Cohen, M. Akhtar, D. Gani, *Biochemistry* **1988**, *27*, 2956–2959.
[8] N. P. Botting, D. Gani, *Biochemistry* **1992**, *31*, 1509–1520.
[9] C. H. Archer, N. R. Thomas, D. Gani, *Tetrahedron: Asymmetry* **1993**, *4*, 1141–1152.
[10] C. H. Archer, D. Gani, *J. Chem. Soc., Chem. Commun.* **1993**, 140–142.
[11] D. Gani, C. H. Archer, N. P. Botting, J. R. Pollard, *Bioorg. Med. Chem.* **1999**, *7*, 977–990.
[12] M. Asuncion, W. Blankenfeldt, J. N. Barlow, D. Gani, J. H. Naismith, *J. Biol. Chem.* **2002**, *277*, 8306–8311.
[13] C. W. Levy, P. A. Buckley, S. Sedelnikova, Y. Kato, Y. Asano, D. W. Rice, P. J. Baker, *Structure* **2002**, *10*, 105–113.
[14] P. C. Babbitt, M. S. Hasson, J. E. Wedekind, D. R. J. Palmer, W. C. Barrett, G. H. Reed, I. Rayment, D. Ringe, G. L. Kenyon, J. A. Gerlt, *Biochemistry* **1996**, *35*, 16489–16501.
[15] The diastereoisomer **2** can be easily distinguished from the diastereoisomer **3** in ^{1}H NMR spectra by examining the chemical shifts for the signals due to the protons of the methyl groups, which occur at ~0.95 and ~1.08 ppm, respectively.
[16] The purchased material used as substrate **2** is actually a 1:1 mixture of the enantiomers (2*S*,3*S*)- and (2*R*,3*R*)-3-methylaspartic acid. The (2*R*,3*R*)-enantiomer is not a substrate nor an inhibitor of MAL. Hence, the maximal yield of **1** in these experiments is 50%.
[17] A pK_a reflecting the α-amino group of **2** is not observed in the log (k_{cat}/K_M) versus pH profile because data were not collected to high enough pH to define such a pK_a. It is important to note that the proposed protonation state of the α-amino group (Schemes 1, 2, 3) is consistent

with the observation that this group occupies a region of the active-site pocket that is solvent exposed.[13]

[18] A comparison of the crystal structures of *C. amalonaticus* MAL (in complex with **2**)[13] and *C. tetanomorphum* MAL (in the absence of a bound ligand)[12] shows that all active-site residues are positionally conserved, although the sidechain orientation of Lys331 is somewhat different. Moreover, modeling of the three-dimensional structure of **2** into the active site of *C. tetanomorphum* MAL by using the X-ray structure of the *C. amalonaticus* MAL in complex with **2** as a guide, gives similar substrate interactions within the two enzyme active sites (data not shown). These observations suggest that both MAL enzymes have a highly similar substrate binding mode and catalytic mechanism.

[19] B. Mitra, A. T. Kallarakal, J. W. Kozarich, J. A. Gerlt, J. G. Clifton, G. A. Petsko, G. L. Kenyon, *Biochemistry* **1995**, *34*, 2777–2787.

[20] J. Sambrook, E. F. Fritsch, T. Maniatis, *Molecular Cloning: A Laboratory Manual*, 2nd ed., Cold Spring Harbor Laboratory Press, New York, **1989**.

[21] W. J. Waddell, *J. Lab. Clin. Med.* **1956**, *48*, 311–314.

[22] N. M. Kamerbeek, M. W. Fraaije, D. B. Janssen, *Eur. J. Biochem.* **2004**, *271*, 2107–2116.

[23] S. N. Ho, H. D. Hunt, R. M. Horton, J. K. Pullen, L. R. Pease, *Gene* **1989**, *77*, 51–59.

[24] A. D. J. MacKerell, B. R. Brooks, C. L. I. Brooks, L. Nilsson, B. Roux, Y. Won, M. Karplus in *Encyclopedia of Computational Chemistry* (Ed.: P. V. Schleyer), Wiley, Chichester, **1998**, pp. 271–277.

[25] J. A. Erickson, M. Jalaie, D. H. Robertson, R. A. Lewis, M. Vieth, *J. Med. Chem.* **2004**, *47*, 45–55.

[26] G. Wu, D. H. Robertson, C. L. Brooks, III, M. Vieth, *J. Comput. Chem.* **2003**, *24*, 1549–1562.

[27] W. L. DeLano, *The PyMOL Molecular Graphics System*, DeLano Scientific, San Carlos, CA, USA, **2002**. (http://www.pymol.org).

Received: May 19, 2009
Published online on August 7, 2009

